

Energy Harvesting from Anti-Corrosion Power Sources

Sehwan Kim
Dept. of Biomed. Engineering
Dankook University, S.Korea
paul.kim@dankook.ac.kr

Minseok Lee
Dept. of Medical Laser
Dankook University, S.Korea
lifeway1972@gmail.com

Pai H. Chou
University of California
Irvine, CA 92697-2625 USA
phchou@uci.edu

ABSTRACT

This work presents energy harvesting techniques from low-voltage current used to prevent galvanic corrosion between a metallic structure and a permanent copper/copper sulfate (Cu/CuSO_4) reference electrode. Supercapacitors are adopted to compensate for or overcome the limitations of batteries. Then, a boost converter is used to convert the low voltage levels of galvanic corrosion to that needed by the complementary metal oxide semiconductor (CMOS) technologies used for the wireless sensor systems. Experimental results show that our proposed harvesting schemes significantly reduce the overhead of the charging circuitry, which enables nearly full charging of supercapacitors of up to 350 F under the low power conditions of 3 mW (i.e., 3 mA at 1 V). More importantly, our system enables maintenance-free operation of remote-monitoring cathodic protection (RMCP) systems in harsh environments, where sunlight or wind power may be unavailable or unpredictable.

Categories and Subject Descriptors

B.0 [Hardware]: General

General Terms

Design, Performance measurement

Keywords

Energy harvesting, galvanic corrosion, cathodic protection systems.

1. INTRODUCTION

Cathodic protection (CP) is the most effective electrical method of controlling and reducing corrosion on metallic structures such as water storage tanks, lock gates and dams, steel pilings, ship hulls and interiors, and water treatment equipment, located underground or underwater. In particular, the CP method has been widely used on the metal pipeline systems for the transmission and distribution of gas, petrochemical, and water [9, 10, 12]. By simply maintaining anticorrosion voltage levels, one can effectively stop corrosion of the metal pipelines.

Permission to make digital or hard copies of all or part of this work for personal or classroom use is granted without fee provided that copies are not made or distributed for profit or commercial advantage and that copies bear this notice and the full citation on the first page. Copyrights for components of this work owned by others than ACM must be honored. Abstracting with credit is permitted. To copy otherwise, or republish, to post on servers or to redistribute to lists, requires prior specific permission and/or a fee. Request permissions from permissions@acm.org.

ISLPED'14, August 11–13, 2014, La Jolla, CA, USA.

Copyright © 2014 ACM 978-1-4503-2975-0/14/08... \$15.00.

<http://dx.doi.org/10.1145/2627369.2627624>.

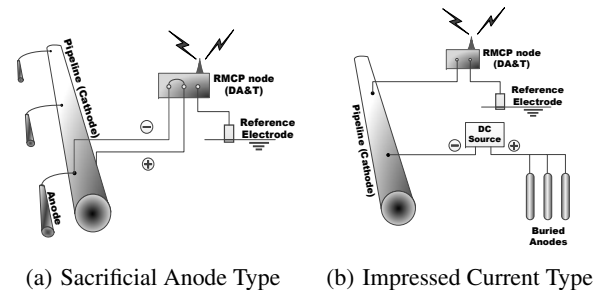


Figure 1: Remote-monitoring Cathodic Protection Systems

1.1 Remote Monitoring of CP Systems

To ensure proper performance of anticorrosion, periodic monitoring of the CP system is required. To be in compliance with National Association of Corrosion Engineers (NACE) guidelines, it is necessary to take and report monthly or bimonthly measurements of the voltage potential between a reference electrode at the various test points [10]. In the conventional monitoring process for CP systems, the measurements are carried out manually using a digital multimeter on the site. These manual measurements not only incur high cost of traveling to remote sites, but they also leave the pipelines unprotected until the fault is discovered by routine measurement.

Remote-monitoring Cathodic Protection (RMCP) systems are those that combine smart corrosion sensors [3, 16] with remote monitoring functions [11, 15]. They have been receiving growing interest in recent years. They automate the data collection process and provide immediate warning of potential corrosion hazards by an RMCP node. Fig. 1 shows the representative RMCP systems with the RMCP nodes for data acquisition and transmission (DA&T): sacrificial anode and impressed current types.

1.1.1 Sacrificial Anode System

The operational principle of the first type is to connect an external anode to the metal structures to be protected, resulting in passing a positive direct current (dc) between them. The metal structure becomes a cathode that does not corrode, while the external anode is corroded. The dc current is used as a protective current by consuming iron of the anode (e.g., activated aluminum, zinc or magnesium). In other words, the anode is sacrificed by corrosion and is therefore named a *sacrificial anode system* as shown in Fig. 1(a). Due to the sacrifice of the anode, the system is required to periodically replace the sacrificed anode.

1.1.2 Impressed Current System

In Fig. 1(b), a dc source is placed between the metal structures and the anode to avoid the replacement cost of the sacrificed anode. This is called an *impressed current system*, whose anode is made durable thanks to the impressed current from the dc source. As a result, the protective current flows from the anode into the metal structures without any sacrifice of the anode.

1.1.3 Monitoring Functions

Whether sacrificial anode or impressed current is used, an RMCP node typically performs three main functions: corrosion sensing, data acquisition, and wireless data transmission [1, 7]. A reference electrode (e.g., Copper/Copper Sulfate (Cu/CuSO₄) or silver/silver chloride (Ag/AgCl)) is inevitable to determine whether it protects the metal structures against corrosion. If the potential of the metal structure against a reference cell is obtained between 850 mV and 2 V, then the corrosion is effectively protected. For CP systems to perform “on-demand” remote monitoring, the node samples the voltage level at the test points on the site and notifies the operation center if the voltage exceeds the threshold level.

1.2 Power Source for RMCP Systems

Most RMCP nodes today are powered by batteries. They are power managed by duty-cycling to extend the battery life, but the battery is still the main limiting factor associated with the RMCP nodes due to non-ideal effects such as the memory effect and the limited number of recharge cycles. As a result, batteries need to be replaced every 1-2 years and incur high replacement cost.

To address these disadvantages of batteries, researchers start proposing the use of supercapacitors, also known as ultracapacitors or electrochemical double layer capacitors (EDLCs), as the type of energy storage element (ESE) of choice. Supercapacitors have extremely long life cycles, high power density, and eco-friendly materials [2, 5, 6]. The voltage difference between an anode and a reference electrode is 0.85 to 2 V while the current varies from 2 to 4 mA depending on the soil condition surrounding a single reference electrode. This level of cumulative energy over time is nontrivial and can be sufficient for running duty-cycled remote-monitoring CP nodes. However, scavenging energy from galvanic corrosion and storing the harvested energy to supercapacitors pose new challenges on designing subwatt-scale harvesters. The voltage between the anode and the reference electrode is not directly usable unless up-converted to CMOS voltage levels, but this incurs nontrivial overhead. Also, the self-discharge (leakage) rate of supercapacitors increases rapidly near their rated voltage and can be similar to or exceed the charging current.

1.3 Contributions

The main contribution of this work is the development of an energy harvesting technique from corrosion energy: the galvanic current induced by the natural voltage difference between a cathode and a reference electrode in the remote-monitoring CP systems. We propose solutions in terms of charging and discharging phases using the supercapacitor-based energy harvester.

First, a *hysteretic charging* scheme is suggested to charge *reservoir supercapacitors* (of large capacitance) under the condition of low ambient power by offsetting the leakage of supercapacitors. The *input supercapacitor* (of small capacitance) accumulates the energy from the low-power ambient source, and then rapidly releases the accumulated energy to the reservoir supercapacitors within the hysteresis band. This charging scheme overcomes the leakage of the reservoir supercapacitors.

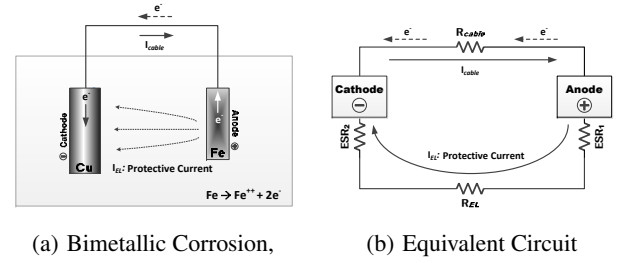


Figure 2: Corrosion Mechanism; where R_{cable} is cable path resistance, R_{EL} is electrolyte path resistance, ESR_1 is apparent or effective boundary resistance at the anode, ESR_2 is apparent or effective boundary resistance at the cathode.

Second, we propose a hybrid supply circuit for our supercapacitor-based system to efficiently power the target embedded loads in both active and low-power modes. Unlike batteries, since the voltage of a supercapacitor drops as the stored energy is released, most supercapacitors need a dc-dc converter to maintain a stable voltage level when driving target loads. However, most dc-dc converters have higher quiescent current than the sleep current of most embedded systems by 2-3 orders of magnitude. Our proposed scheme can eliminate most of the quiescent current by adding the near-constant voltage ESE for powering the load during sleep mode.

The remainder of this paper is organized as follows. Section 2 first provides theoretical background on galvanic corrosion and the characteristics of supercapacitors. We also survey current RMCP systems with energy harvesting. Section 3 describes the architecture of the harvesting system and the critical schemes. Section 4 presents the system specification and a working prototype of the proposed harvester. Section 5 presents the evaluation results of our hysteretic harvesting scheme for the RMCP system. Section 6 concludes the paper with directions for future work.

2. BACKGROUND AND RELATED WORK

Metal in the extraction from its ore has a natural tendency to revert to its original state under the action of oxygen and water. This action is called corrosion and the most common example is rusting [13]. Corrosion is an electro-chemical process related to the electrical currents on a micro or macro scale. This corrosion process is produced by the natural potential difference in galvanic couples, or the variations at different points on the surface of metallic structures such as pipeline systems. To initiate the electro-chemical process, the following four components must be included: anode, cathode, electrolyte, and connecting conductor, as shown in Fig. 2. Corrosion normally occurs at the anode but not the cathode.

2.1 Galvanic Corrosion

Galvanic corrosion (i.e., bimetallic corrosion) generates the galvanic current by connecting two dissimilar metals buried in the electrolyte such as soil. Most soils contain moisture and mineral salts and therefore make a good electrolyte. Fig. 2(a) describes the galvanic current resulting from the connection of two dissimilar metals submerged in the electrolyte. If a copper and a metal (e.g., Fe) are electrically connected in the soil, the electrolytic nature of the soil gives rise to a galvanic action in which the copper acts as a cathode and the metal as an anode. In this closed circuit, the protective current (direct current) will flow through the soil from the metal to the copper. Metal ions leave the anode by way of the electrolyte, and electrons travel from the anode to the cathode by way

of the cable connection path. This galvanic corrosion occurs only at the anode (Fe) while the cathode (copper) is protected. Fig. 2(b) shows the equivalent circuit for the galvanic current loop. The current flows are a result of potential difference (i.e., $I_{\text{cable}} \cdot R_{\text{cable}}$) between the anode and the cathode. The amount of current (I_{cable} or I_{EL}) flowing in galvanic couples depends on the magnitude of the driving voltage and the total effective resistance. This electrical behavior can be equally applied to the galvanic corrosion between metallic structures and the reference electrode.

2.2 Characteristics of Supercapacitors

Supercapacitors can be an excellent ESE for the harvesters, due to their power density and durability. However, in such systems, the non-ideal behavior attributed to substantial *leakage currents* and *charge redistribution* inside the supercapacitors need to be addressed [2, 17]. The charge redistribution can be reduced by repeating several charging-discharging cycles in the initial phase. However, the leakage current can still be considerable and is inevitable. According to the literature on supercapacitors modeling, their leakage power grows rapidly with the size (i.e., capacitance) and with the remaining energy. For example, at 2.5 V, the leakage power of 22 F, 100 F, and 300 F supercapacitors is 2 mW, 7 mW, and 17 mW, respectively. When the leakage power of the supercapacitor at a given voltage is higher than the ambient power of the RMCP system (at 3 mW), the RMCP system is actually at a loss. Therefore, the leakage rate should be capped by limiting the capacitance of supercapacitors, by limiting the voltage, or both. To overcome these limitations, we propose a *hysteretic charging* scheme, which is helpful to extend the upper bound on the capacitance of supercapacitors.

2.3 RMCP Systems with Energy Harvesting

Energy harvesting techniques for RMCP systems have been explored and studied extensively by researchers. The research approaches varied in their remote monitoring techniques, the types of CP systems, and data acquisition methods.

Mishra et al. [8] introduced Solar Photovoltaics (SPV) instead of a dc power source of the impressed-current CP system. Since the output of the SPV is a dc voltage, it can eliminate the rectifier that is found in conventional impressed CP systems. The SVP-based CP system simply replaces the dc power source of the conventional CP system with SVP power; it does not support DAQ and remote monitoring function, so routine manual inspection is still required.

Ghitani et al. [4] presented a prototype microprocessor-based CP system employing a photovoltaic (PV) power source. The PV array generates dc power from solar irradiation, and a microprocessor-controlled unit enables the impressed current to make automatic adjustments according to the state of corrosion of the pipeline. However, since the pipelines generally run through inaccessible remote locations, the PV power source would not be suitable for supplying stable power to the RMCP system.

Sun et al. [14] provided a corrosion-monitoring sensing framework based on the Mica mote for *reinforcing concrete* (RC) structures. The Mica mote is duty-cycled in conjunction with routing policy to extend the lifetime of the monitoring unit. However, this system uses a lithium battery, which typically requires replacement every 1-2 years.

3. HARVESTING SYSTEM DESIGN

We propose a system that harvests energy from the RMCP environments. The typical ambient power is around 3 mW, making it challenging to harvest. We define the following requirements. First, the total power budget of the harvester itself is 1 mW

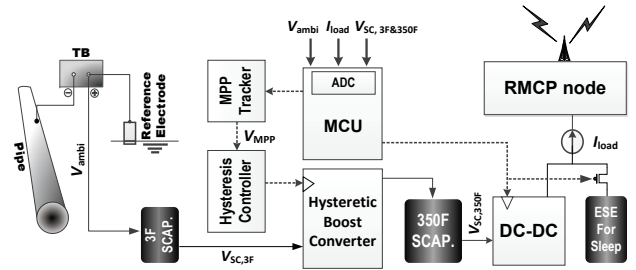


Figure 3: System block diagram for an ultra-low power consumption harvester.

max. Second, the output current of the charger should be higher than the leakage of supercapacitors. Third, the dc-dc converter on the output stage of the harvester must have very low quiescent current. To solve these problems, we propose a supercapacitor-based, hysteretic-charging energy-harvesting system named Hys-Cap, whose block diagram is shown in Fig. 3.

3.1 Hysteretic Charging Scheme

The minimum conversion voltage ($V_{\text{conv, min}}$) of most boost-up dc-dc converters to date is 0.7 V [18]. The dc-dc converters operate most efficiently when the input and output voltages are similar, but when boosting from 0.7 V to 3 V, they operate at $\leq 30\%$ efficiency. To ensure $\geq 75\%$ efficiency while considering the minimum voltage of the ambient source, the input voltage of the charger should be ≥ 0.9 V at the output voltage of 3 V. As shown in Fig. 3, given the available power of 3 mW (i.e., 3 mA at 1 V) to harvest and the charger efficiency of 75%, the output current from the charger is 0.75 mA. According to references in the literature on supercapacitors, the leakage power of supercapacitors increases exponentially with the capacitance and the (open-circuit) voltage of the supercapacitors. As their voltage approaches their rated voltage (e.g., 2.3 or 2.7 V), their leakage current can be too high such that charging will result in a net loss. For instance, the leakage current of 300 F supercapacitors is around 15 mA at 2.5 V. To charge up to 2.4 V at the charging current of 0.75 mA with a net gain, a single supercapacitor should be kept no larger than 10 F.

To overcome the high leakage issue, as well as to increase the chargeable size of supercapacitors, we propose the new scheme called *hysteretic charging*. First, the ambient source charges a smaller capacitor on the input. When it approaches the preset voltage (1 V), the charger is turned on and then starts to transfer the stored energy to the reservoir supercapacitor (350 F) until the voltage of the input supercapacitor drops by 0.1 V, which is in the hysteresis range. This technique ensures that the efficiency of the charger remains above 75% by fixing the input voltage of the charging between 0.9 V and 1 V. Furthermore, this scheme can transfer higher current than the leakage current of reservoir supercapacitors, so that it can effectively charge larger supercapacitors than those charged by the conventional continuous charging scheme.

3.2 Discharging Control

Due to the low nominal rated voltage of supercapacitors (e.g., 2.3 V or 2.7 V), most supercapacitor-based harvesters need a dc-dc converter to supply the specified voltage of the target embedded system. Buck/boost regulators are commonly used for converting a supercapacitor's lower voltage to the given target voltage. The typical target embedded system has two modes of operation: active

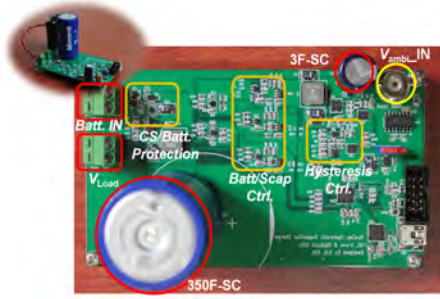


Figure 4: Prototype of HysCap harvester for an RMCP node

Table 1: Power consumption of components of HysCap

	Status	Power Consumption	Part Number
Microcontroller	Active	4 mA@3 V	C8051F960
	Sleep	600 nA@3 V	
Boost Converter	I_Q	1 μ A	AS1310
Hys. & MPPT	I_Q	3.3 μ A	AD8603, LT6656
	$I_{shutdown}$	< 1 μ A	
DC-DC	I_Q	55 μ A	TPS61200
Current Sensor	I_{supply}	0.75 μ A	MAX9610

and sleep. For our application domain, the range of power consumption in active mode is from 100 to 150 mW, while in sleep mode, the power consumption ranges from 1.8 mW (3.6 V/0.5 mA) to 12.5 mW (5 V/2.5 mA), where the efficiency of a load-side dc-dc converter drops to 5%. This means 36 mW is drawn from a reservoir supercapacitor to supply 1.8 mW to the target embedded loads. In other words, the efficiency of the load-side dc-dc converter can be a crucial problem when the target load is in sleep mode.

To address the efficiency problem in sleep mode, we propose to add ESEs to power the load during sleep mode without going through the load-side dc-dc converter, which drives the load during active mode only. As shown in Fig. 3, a current sensor detects whether the target embedded load is in active or sleep mode. When in sleep mode, the current sensor outputs a low level (logic '0'), which disables the load-side dc-dc converter during sleep mode. When either the current sensor detects the high current in active mode or the voltage of the additional EHSs drops to the required minimum voltage of the target embedded loads, the load-side dc-dc converter is turned on. This discharging scheme should be able to eliminate the inefficiency of the load-side dc-dc converter during sleep mode of the target load.

4. IMPLEMENTATION

This section describes a prototype harvesting system named HysCap for an RMCP systems. The requirements for our harvester was derived from the availability of ambient power at an actual RMCP site and the power consumption of a commercial RMCP node.

4.1 System Requirements

The ambient sources are characterized as follows. The potential on the conductive wire is around 850 mV relative to a Cu/CuSO₄ reference electrode, and the current density from reference electrode is 2 to 4 mA depending on the soil condition surrounding a single reference electrode. Next, the power consumption of the RMCP node is measured to design the output-stage circuitry of HysCap. The power consumption of the RMCP node (DART, by Borin, USA) is 126 mW (35mA at 3.6V) in active mode and 0.65 mW (0.18mA at 3.6V) in sleep mode. In fact, the 0.18 mA

is the *root mean square* (RMS) current, since sleep mode consists of a sequence of periodical catnap signals. The duty cycle to monitor the potential between a wire connected to pipelines and the Cu/CuSO₄ reference electrode is 1%.

Therefore, the HysCap harvester should be designed with < 1 mW of overhead when charging the large reservoir supercapacitor under the lower ambient-power condition. It should store a sufficient amount of energy to power the RMCP node at 35 mA/3.6 V for the 1% duty cycle of continuous RF transmission for one hour, plus 0.18 mA/3.6 V during sleep mode of the RMCP node for 98% of the time (i.e., charging time = 96 hours, or 4 days).

4.2 Harvesting System

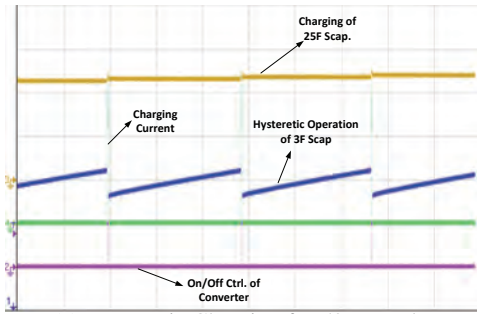
The proposed hysteretic charging and discharging system has been implemented using COTS parts. The boost converter (AS1310) has built-in hysteresis function and ultra-low quiescent current (I_Q) of 1 μ A. The hysteresis band can be extended by adjusting the external resistive voltage divider, resulting in the lower-bound voltage of 0.9 V and upper-bound voltage of 1 V. As mentioned in Section 1, the voltage and the current of the ambient sources from RMCP systems can vary depending on soil conditions. Thus, the charger needs to track the maximum power point (P_{MPP}) from the RMCP environment. The microcontroller unit (MCU) detects the change of the open-circuit voltage (V_{oc}) between an anode and a reference electrode. If the voltage varies by more than 0.2 V, the MCU is waken up by the interrupt signal and moves the center voltage of the hysteresis band by adjusting the digital potentiometer on the resistive voltage divider. By setting the hysteresis band to 0.9 - 1 V, the efficiency of the buck converter can be increased.

The current sensor monitors the load current to detect whether the RMCP node is in active or sleep mode. According to Table 1, the overall power consumption of the proposed harvester is 0.46 mW at 1% duty cycle. Considering the harsh environmental conditions, both the NEMA 4+ enclosure and the conformal coating made of modified polyurethane resins (PUR) are applied to the harvester for the RMCP system. The enclosure helps protect the harvester against heavy rain, high humidity, and high temperature, while the conformal coating insulates the assembled printed circuit boards (PCBs) from the harsh environment.

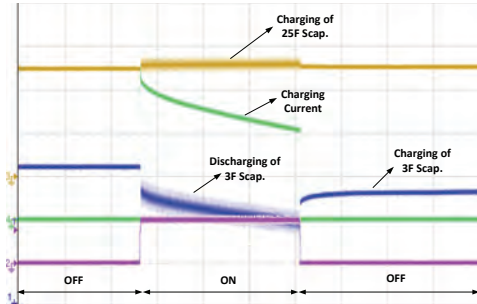
5. EVALUATION

To validate the proposed charging scheme, we set up the experiment using a 3 F input supercapacitor and a 350 F reservoir supercapacitor (BCAP0350). The power of the ambient source is simulated using a regulated power supply set at 1 V/3 mA based on conditions at a representative deployment site. The hysteresis window size is 100 mV; that is, the hysteresis range is preset from 1 V to 0.9 V of the 3 F input supercapacitor.

The typical boost converter continuously transfers the charged energy of an input ceramic capacitor to either the load or ESEs. Since the value of the input capacitor is related to the efficiency and the amount of ripple of the boost converter, tens or hundreds of microfarad is usually suitable capacitance on the input. However, considering supercapacitors as a reservoir ESE, in case of low ambient power condition, it is difficult to charge supercapacitors of large capacitance due to high leakage current. To compensate for or overcome the high leakage current, we replace the input ceramic capacitor with a 3 F supercapacitor. In this experiment, we assume that the ambient source outputs power at 1 V/3 mA. Accordingly, the maximum power point (MPP) of the ambient source can be 0.95 V considering the built-in hysteresis band of 100 mV. In other words, the MPP tracker adjusts the center voltage V_{MPP} of the hysteresis comparator to 0.95 V.



(a) Hysteretic Charging for 50 seconds.



(b) Zoomed-In View of Charging.

Figure 5: Oscilloscope Snapshots showing Charging Phase of HysCap.

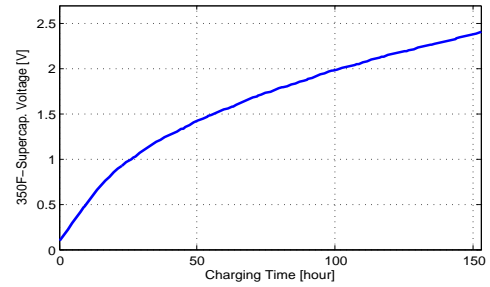
Once the voltage of the 3 F supercapacitor approaches 1 V (i.e., $V_{MPP} + V_{Hysteresis}$), the hysteresis controller turns on the boost converter and then transfers the stored energy of the 3 F input supercapacitor to the 350 F reservoir supercapacitor. After transferring the stored energy, the voltage of the 3 F supercapacitor drops to $V_{MPP} - V_{Hysteresis}$ (≈ 0.9 V). At that point, the hysteresis controller turns off the boost converter, causing the 3 F supercapacitor to start accumulating energy from the ambient source until its voltage exceeds $V_{MPP} + V_{Hysteresis}$ again.

Fig. 5 summarizes how the hysteresis operation works in the prototype energy harvester. At this moment, we use the combination of 3 F input supercapacitor and 25 F reservoir supercapacitor to show clearly the hysteretic operation based on the display range of the oscilloscope. The boost converter turns on and delivers the stored energy from the 3 F input supercapacitor to the 25 F reservoir supercapacitor at the rate of 550 mA (green solid line) for the short duration of 340 ms instantaneously. As soon as the 3 F supercapacitor's voltage (blue solid line) reaches the lower bound of the hysteretic window, the boost converter turns off (purple solid line), and the ambient source starts to charge the 3 F input supercapacitor again up to the upper bound of the hysteretic window.

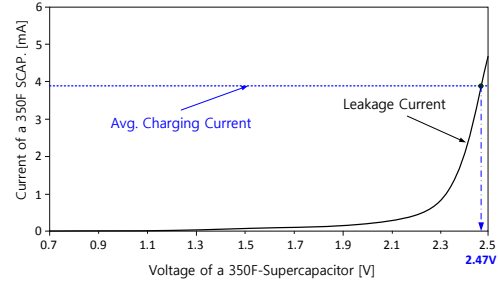
5.1 Charging Phase

According to the data sheet of the BCAP0350, the leakage current of the 350 F supercapacitor is 0.30 mA, which is measured after 72 hours at 25°C and rated voltage. This means that initially, the leakage current can be much higher than that reported by the data sheet.

To accurately characterize the leakage current of the 350 F supercapacitor, we perform measurement. The average charging current during one charging cycle of 140 seconds is 3.93 mA, which is higher than the leakage current of 3.5 mA at 2.4 V of the 350 F supercapacitor. Therefore, the 350 F reservoir supercapacitor can



(a) Charging the reservoir supercapacitor



(b) Average Charging Current vs. Leakage current of the 350F Supercap.

Figure 6: Measured Charging Voltage of 350 F.

also be charged under the low ambient-power source of 1 V/3 mA by the benefit of the proposed hysteretic charging scheme.

Fig. 6(b) delineates the measured leakage current of the 350 F supercapacitor and the average charging current of the hysteretic charging scheme. In this figure, the crossing point of the two lines indicates the maximum charging voltage of the 350 F supercapacitor using the proposed hysteretic charging scheme.

Fig. 6 shows the measured voltage based on the combination of a 3 F input supercapacitor and a 350 F reservoir supercapacitor by the 100 mV hysteresis window. Fig. 6(a) shows the 350 F one that has been charged to 2.0 V after about 4 days. The 350 F reservoir supercapacitor is eventually charged while alternating between a higher charging rate and a lower self-discharging rate. As the voltage of the supercapacitor approaches the maximum chargeable voltage, the leakage current increases rapidly, and therefore the charging rate decreases.

6. CONCLUSIONS AND FUTURE WORK

We have shown the feasibility of our proposed supercapacitor-charging scheme by validating its functions: hysteresis, current delivery, and charging capability. The experimental results show that the proposed scheme can charge supercapacitors of up to 350 F, larger than the upper bound of 2 F in series achieved by all previous COTS chargers at this very low power level (e.g., LTC3625, Linear Technology). As a result, this scheme makes it possible to implement the supercapacitor-based energy harvester under the low ambient power conditions. That is, the proposed scheme enables supercapacitors to be used as a reservoir energy storage element. In short, the proposed charging scheme will enhance the charging ability under the low-power ambient source and improve the charging efficiency.

Future work includes system-level optimizations. The hysteretic window size will be explored to maximize the power-conversion efficiency of the dc-dc converter. Besides, the dedicated MCU of the prototype harvester can be eliminated by either moving its functions to an existing MCU, such as the one on the RMCP node or by adding logic circuitry. Finally, we are planning to install our proposed harvesting system to validate its performance in the short term and eventually deploy an improved design for the long term.

7. REFERENCES

- [1] Mohammed Zeki Al-Faiz and Liqaa Saadi Mezher. Cathodic protection remote monitoring based on wireless sensor network. *Wireless Sensor Network*, 4(7):226–233, September 2012.
- [2] Davide Brunelli, Clemens Moser, Lothar Thiele, and Luca Benini. Design of a solar-harvesting circuit for batteryless embedded systems. *IEEE Transaction on Circuits and Systems I: Regular Papers*, 56(11):2519–2528, November 2009.
- [3] Andy Cranny, Nick R. Harris, Mengyan Nie, Julian A. Wharton, Robert J. K. Wood, and Keith R. Stokes. Sensors for corrosion detection: Measurement of copper ions in 3.5% sodium chloride using screen-printed platinum electrodes. *IEEE Sensors Journal*, 12(6):2091–2099, June 2012.
- [4] H. El Ghitani and A. H. Shousha. Design of a solar photovoltaic-powered mini cathodic protection system. *Journal of Applied Energy*, 52(2-3):299–305, September 2000.
- [5] Sehwan Kim and Pai H. Chou. Energy harvesting by sweeping voltage-escalated charging of a reconfigurable supercapacitor array. In *Proceedings of International Symposium on Low Power Electronics and Design (ISLPED)*, pages 235–240, Fukuoka, Japan, August 1-3 2011.
- [6] Sehwan Kim and Pai H. Chou. Size and topology considerations for supercapacitor-based micro-solar harvesters. *IEEE Transactions on Power Electronics (TPEL)*, 28(4):2068–2080, April 2013.
- [7] A. Kumar and L. D. Stephenson. Comparison of wireless technologies for remote monitoring of cathodic protection systems. Technical report, U.S. Army Corps of Engineers, Engineer Research and Development Center Construction Engineering Research Laboratory, Champaign, USA, 2007.
- [8] P.R. Mishra, J.C. Joshi, and B. Roy. Design of a solar photovoltaic-powered mini cathodic protection system. *Solar Energy Materials and Solar Cells*, 61(11):383–391, September 2000.
- [9] M. Mohitpour, H. Golshan, and A. Murray. *Pipeline Design and Construction: A Practical Approach (3rd Edition)*. American Society of Mechanical Engineers (ASME) PRESS, 2007.
- [10] A. W. Peabody. *Peabody's Control of Pipeline Corrosion (2nd Edition)*. Houston, TX, USA, January 2001.
- [11] Guofu Qiao, Clemens Moser, Yi Hong, Yuelan Qiu, and Jinping Ou. Remote corrosion monitoring of the RC structures using the electrochemical wireless energy-harvesting sensors and networks. *Journal of NDT&E International*, 44(7):583–588, June 2011.
- [12] Douglas P. Rieme. *Modeling cathodic protection for pipeline networks*. PhD thesis, University of Florida, 2000.
- [13] Pierre R. Roberge. *Corrosion Engineering: Principles and Practice*. The McGraw-Hill companies, 2008.
- [14] Guodong Sun, Guofu Qiao, and Bin Xu. Corrosion monitoring sensor networks with energy harvesting. *IEEE Sensors Journal*, 11(6):1476–1477, June 2011.
- [15] Yan Yu, Guofu Qiao, and Jinping Ou. Self-powered wireless corrosion monitoring sensors and networks. *IEEE Sensors Journal*, 10(12):1901–1902, December 2010.
- [16] Yan Yu, Guofu Qiao, and Jinping Ou. Optimization design of a corrosion monitoring sensor by fem for rc structures. *IEEE Sensors Journal*, 11(9):2111–2112, September 2011.
- [17] Ting Zhu, Yu Gu, Tian He, and Zhi-Li Zhang. eShare: A capacitor-driven energy storage and sharing network for long-term operation. In *Proceedings of the 8th ACM Conference on Embedded Networked Sensor Systems*, pages 239–252, Zurich, Switzerland, November 3-5 2010.
- [18] Ting Zhu, Ziguang Zhong, Yu Gu, Tian He, and Zhi-Li Zhang. Leakage-aware energy synchronization for wireless sensor networks. In *Proceedings of the 7th international conference on Mobile systems, applications, and services (MobiSys)*, pages 319–332, Kraków, Poland, June 22-25 2009.